JSST
Journal of Space Science and Technology

P-ISSN: 2008-4560
E-ISSN: 2423-4516

Journal of Space Science and Technology

Vol. 17, Special Issue, pp. 59-65, 2024
https://doi.org/10.22034/jsst.2024.1518
Journal Homepage: https://jsstpub.com

Original Research Paper

Designing an Adaptive Velocity Obstacle Avoidance System for Autonomous Mars Rover Navigation in Dynamic Terrains

Karim Ahmadi Dastgerdi[1*], Seyedeh Marziyeh Salehi Ghahfarokhi[2], and Sadegh Ahmadi Dastgerdi [3]

1. School of Architecture, Technology and Engineering, University of Brighton, Brighton, UK
2. University of Brighton, Brighton, UK
3. Basir Andishan Bina Tadbir, Tehran, Iran

ARTICLE INFO

Article History:

Received 06 November 2024
Revised 16 December 2024
Accepted 16 December 2024
Available Online 16 December 2024

Keywords:

Adaptive cone
Autonomous navigation
Collision avoidance
Mars rover
Obstacle avoidance
Space vehicle

ABSTRACT

Over the past decade, various velocity obstacle-based methodologies have been developed for collision avoidance in dynamic environments. However, these methods are often limited to handling only a few obstacles, sequential encounters, or lack of safety guarantees in complex, unstructured terrains. This paper proposes an adaptive collision avoidance strategy using the velocity obstacle method, designed to enable autonomous Mars rovers to safely navigate dynamic and uncertain terrains while avoiding multiple obstacles simultaneously. The strategy constructs an adaptive velocity cone, accounting for dynamic obstacles and terrain features, ensuring continuous safety while guiding the rover to its waypoint. We implement the strategy in simulated Mars exploration scenarios that represent challenging multi-obstacle tasks. The simulation results demonstrate that our approach enhances performance by increasing safety distances, making it highly suitable for autonomous planetary exploration, where collision avoidance is critical for mission success.

* Corresponding Author's E-mail: k.ahmadidastgerdi@Brighton.ac.uk

How to Cite this Article:
K. Ahmadi Dastgerdi, S. M. Salehi Ghahfarokhi, and S. Ahmadi Dastgerdi, "Designing an adaptive velocity obstacle avoidance system for autonomous Mars rover navigation in dynamic terrains," *Journal of Space Science and Technology*, Vol. 17, Special Issue, pp. 59-65, 2024, https://doi.org/10.22034/jsst.2024.1518.

1. INTRODUCTION

Autonomous systems play a pivotal role in modern applications, facilitating automation and efficient operation in dynamic and uncertain environments. These systems operate through loops that govern control and decision-making processes. The inner loop focuses on implementing a controller to ensure system stability and achieve desired performance, while the outer loop is dedicated to path planning and guidance algorithms that determine feasible paths and direct the system effectively.

In recent years, control strategies for dynamic systems operating in uncertain environments have evolved significantly. These approaches, discussed in [1–3], address challenges such as external disturbances, modeling inaccuracies, and unknown conditions. In Refs. [4, 5] adaptive control strategies for satellites are developed. The controllability of dynamic systems under various uncertainties has also been extensively studied [6]. A predictive controller is for spacecraft is introduced in Ref. [7]. For outer-loop controllers, advancements have been made in optimizing path planning and guidance to enhance efficiency and robustness, as highlighted in [8,9].

Collision avoidance is a crucial aspect of autonomous Mars Rover (MR) navigation, enabling safe exploration of unstructured and challenging Martian terrains. It minimizes the risk of damage to sensitive equipment and scientific instruments, safeguards mission success, optimizes energy consumption—a critical factor for power-limited rovers—and ensures continuous data collection, maximizing the scientific value of the mission. While many studies have explored path-planning methods [10, 11], integrating collision decision-making and reactive obstacle avoidance in dynamic and uncertain environments remains relatively underexplored.

High-speed ships present a parallel case, where collision avoidance algorithms have been developed to address dynamic movement and decision-making challenges [12–14]. Insights from these maritime systems have potential applications in MR navigation, highlighting the interdisciplinary nature of the field and the transferability of advancements across domains.

For planetary navigation, methodologies addressing static and semi-dynamic obstacles have been developed [15]. Traditional methods like artificial potential fields (APFs) [16] and optimization-based techniques often struggle in multi-obstacle scenarios. APF methods, for instance, are susceptible to local minima traps and offer limited solutions constrained by predefined cost functions. Similarly, control barrier functions [17, 18] provide theoretical safety guarantees but are computationally intensive and difficult to implement for adaptive planetary navigation.

Multi-vehicle collision avoidance strategies, as demonstrated in [19–22], are typically tailored for structured environments, limiting their applicability to the unpredictable Martian landscape. Recent approaches, such as model predictive control (MPC) [23] and machine learning techniques [24], have shown promise in generating efficient collision-free paths. However, these methods rely heavily on computation and training data, posing challenges for resource-constrained Mars missions.

Reactive collision avoidance algorithms like constant bias and constant angle methods [25] are widely used in robotics and vehicle navigation but require precise tuning of avoidance angles. Improper tuning can lead to inefficiencies or unsafe maneuvers, making them less suitable for dynamic, multi-obstacle scenarios.

The velocity obstacle (VO) algorithm, commonly used in robotics, identifies unsafe velocities leading to collisions. Variants of VO have been applied successfully in underwater [26], aerial [27], and ground robotics [28]. However, conventional VO methods struggle in scenarios with multiple dynamic obstacles due to static cone formulations. Dynamic changes in velocity cone intersections during maneuvers can compromise safety and efficiency.

To address these limitations, we propose an adaptive velocity obstacle (AVO) algorithm combined with a line-of-sight (LOS) guidance law for MR navigation. The LOS guidance ensures the rover remains on course toward its target waypoint, while the AVO algorithm dynamically constructs adaptive velocity cones based on nearby obstacle motions to ensure safety. The proposed system seamlessly switches between target-reaching and collision-avoidance modes, guided by risk assessments involving metrics like the distance to the closest point of approach (DCPA) and time to the closest point of approach (TCPA).

Simulations validate the proposed method, demonstrating its superior performance in handling multi-obstacle scenario compared to existing VO approaches. The remainder of the paper introduces the MR dynamic model and reviews the conventional VO algorithm. It then presents the main results and analyzes the proposed method's performance through simulated scenarios, concluding with key findings and future research directions.

1. 1. Mars Rover Dynamics

We consider the dynamics of an MR as follows:

$$\begin{aligned} \dot{x}(t) &= v_r \cos(\psi(t)), \\ \dot{y}(t) &= v_r \sin(\psi(t)), \\ \dot{\psi}(t) &= -c\psi(t) + c\tau(t), \end{aligned} \tag{1}$$

where the states $(x, y, \psi) \in \mathbb{R}^2 \times \mathbb{S}^1$ represent the position and heading angle of the rover, and $\tau \in \mathbb{R}$ is the input steering command. The position of the rover is denoted as $p_r(t) = [x(t), y(t)]^\top$, $\psi(t)$ represents the heading angle, v_r is the constant velocity, and c is a system parameter. Let $\mathbb{R}$ denote the set of real numbers, $\mathbb{S}^1$ represent the set of real numbers modulo 2π, and $|\cdot|$ denote the Euclidean norm. The notation $\arg\min$ is used to identify the argument of the minimum value of a function. For example, for $x \in \Omega$, $\arg\min_x f(x)$ identifies the points x where $f(x)$ achieves its minimum value.

This dynamic model captures the motion of an MR traversing challenging terrains at a constant velocity. The rover's behavior is modeled as a simplified system suitable for analyzing collision avoidance and path-planning strategies. Figure 1 illustrates an example of a Mars exploration rover used in simulation studies.

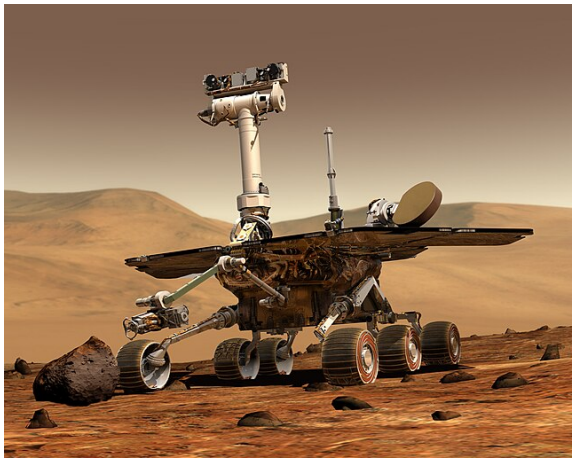

Fig. 1. Illustration of a Mars Exploration Rover.

2. VELOCITY OBSTACLE (VO) METHOD FOR COLLISION AVOIDANCE

The velocity obstacle (VO) method identifies a set of velocities that would lead to a future collision between a MR and an obstacle. By ensuring the MR's velocity remains outside this set, it can effectively avoid collisions [29]. While the obstacle can have any shape, for simplicity, it is assumed to be circular with radius R_o.

The dynamics of a moving obstacle are defined as:

$$\begin{aligned} \dot{x}_m(t) &= v_o \cos(\psi_m), \\ \dot{y}_m(t) &= v_o \sin(\psi_m), \\ \psi_m &= \gamma, \end{aligned} \tag{2}$$

where $(x_m, y_m, \psi_m) \in \mathbb{R}^2 \times \mathbb{S}^1$ represents the obstacle's position and heading, and γ is a constant heading angle. The instantaneous position of the moving obstacle is given by $p_m(t) = [x_m(t), y_m(t)]^\top$, ψ_m is its constant heading angle, and v_o is its constant velocity.

The velocity cone, which geometrically represents the collision region between the MR and a moving obstacle with radius R_o, is illustrated in Figure 2. The edges of the velocity cone are defined by the angles:

$$\psi_v = \psi_d \pm \beta, \tag{3}$$

where ψ_d is the desired heading angle towards the waypoint, and β is the avoidance angle from the obstacle. For a starboard maneuver, $\psi_v = \psi_d + \beta$, and for a port-side maneuver, $\psi_v = \psi_d - \beta$.

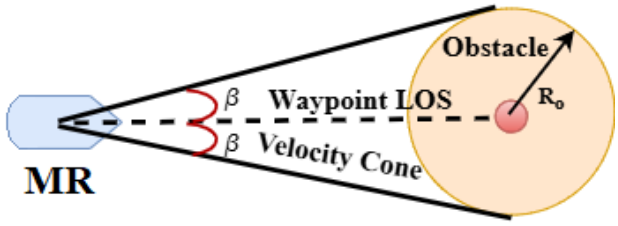

Fig. 2. Velocity cone from the MR to the obstacle.

2. 1. DCPA and TCPA Calculations ([13])

The Distance at Closest Point of Approach (DCPA) is the minimum distance between the MR and the obstacle at their Closest Point of Approach (CPA). The Time to Closest Point of Approach (TCPA) is the time taken for either the MR or the obstacle to reach this CPA, where they are at their minimum distance from each other.

Mathematically, the DCPA and TCPA are given as:

$$\text{DCPA} = \|D\| \sin(\phi), \tag{4}$$

$$\text{TCPA} = \frac{v_r^\top D}{\|v_r\|^2 |\cos(\phi)|}, \tag{5}$$

where:

- $\phi = \cos^{-1}\left(\frac{v_r^\top D}{\|v_r\| \|D\|}\right)$,

- $v_r = [\dot{x} - \dot{x}_m, \dot{y} - \dot{y}_m]^\top$ is the relative velocity,
- $D = [x - x_m, y - y_m]^\top$ is the relative position vector.

3. ADAPTIVE VELOCITY OBSTACLE AVOIDANCE

The Adaptive Velocity Obstacle (AVO) collision avoidance method is integrated with the Line of Sight (LOS) based goal-reaching guidance law. Consequently, the control system for the MR operates in two modes: 1) Target Reaching Mode and 2) Collision Avoidance Mode. The transitions between these modes are determined by decision-making processes based on risk assessment, as discussed in Section **3. 3.** We assume that a sequence of waypoints is provided by the mission planner.

3. 1. Target Reaching Mode

In this subsection, the guidance law for waypoint reaching is described.

Target Reaching Guidance Law

To reach the waypoint $p_t := (x_t, y_t)$, we define the desired guidance law (heading angle) for equation (3) as:

$$\psi_d(t) = \text{atan2}\left((y_t - y), (x_t - x)\right). \tag{6}$$

We define the heading track error as $e(t) = \psi(t) - \psi_d(t)$. Thus, the error dynamics become:

$$\dot{e}(t) = -c\psi(t) + c\tau(t) - \dot{\psi}_d(t). \tag{7}$$

We propose the control law:

$$\tau(t) = \frac{1}{c}\dot{\psi}_d(t) + \psi_d(t), \tag{8}$$

to ensure the asymptotic stability of the heading track error dynamics (7).

3. 2. Obstacle Avoidance Mode

In this mode, the MR avoids multiple dynamic obstacles as follows.

We consider M dynamic obstacles, where the i-th obstacle is represented by the obstacle dynamics in equation (2), with subscripts such as $(x_{mi}, y_{mi}, \psi_{mi}, p_{mi})$ for $i = 1, \ldots, M$. The minimum allowable distance around the obstacle p_{mi} is denoted as C_s, representing the smallest acceptable bound on the DCPA.

We observe that there always exists a change of variables that aligns the waypoint LOS with the x-axis. We now define a criterion for constructing a circle $C(t)$, shown in Figure 3, as follows. Initially, we assume that the circle $C(t)$ with radius $R(t)$ encompasses all dynamic obstacles.

(1) Compute $d_{mi}(t) = \|p_s(t) - p_{mi}(t)\|$. If $d_{mi}(t) < d_{safe} = C_s$, the i-th obstacle $p_{mi}(t)$ is inside $C(t)$;
(2) Compute $d_{mij}(t) = \|p_{mi}(t) - p_{mj}(t)\|, i \neq j$. If $d_{mij}(t) \leq 2d_{safe}$, the j-th obstacle $p_{mj}(t)$ is inside $C(t)$;
(3) Calculate $(TCPA_k, CPA_k)$ according to equation (4) for all $k = 1, \ldots, M$. If $\|p_s(t) - CPA_k\| < d_{safe}$, the k-th obstacle $p_{mk}(t)$ is inside $C(t)$;
(4) If the minimum k exists such that $\|p_s(t) - CPA_k\|$ is minimized at $(CPA_d, TCPA_d)$, compute the new future position of the k-th obstacle $p_{mkl} : (x_{mk}(TCPA_d), y_{mk}(TCPA_d))$ at $TCPA_d$. If $\|p_s(t) - p_{mkl}\| < d_{safe}$, then the l-th obstacle $p_{ml}(t)$ is inside $C(t)$.

After these steps, if there are Q obstacles inside the circle $C(t)$, the radius $R(t)$ is given by:

$$R(t) = \max\{W(t), H(t)\},$$

where $H(t) = \max\{|y_{mq}(t)|\} + C_s$, and $W(t) = \max\{|x_{mq}(t) - x_{mc}(t)|\} + C_s$, with $q = 1, \ldots, Q$, and $p_{mc}(t) : (x_{mc}(t), y_{mc}(t))$ is the CPA_d of the q-th obstacle at which $\arg\min_{k=1,\ldots,M} \|p_s(t) - CPA_q\|$ exists.

In Figure 3, we consider $Q = 3$, and obstacle 3's CPA, $p_{m3c}(t)$, has the minimum distance to the MR $p_s(t)$. Therefore, $p_{m3c}(t) : (x_{m3c}(t), y_{m3c}(t))$ is CPA_d, with $H(t) = |y_{m2}(t)| + C_s$, $W(t) = |x_{m1}(t) - x_{m3c}(t)| + C_s$, and $d_s(t) = \|p_s(t) - p_{m3c}(t)\|$ being the distance between $p_{m3c}(t)$ and the MR $p_s(t)$. The radius of the circle is $R(t) = \max\{W(t), H(t)\}$.

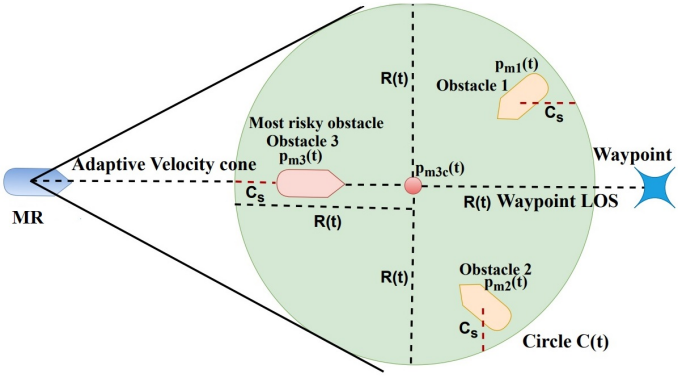

Fig. 3. Illustration of the adaptive velocity cone with multiple obstacles present.

Once the construction of circle $C(t)$ is complete, the desired heading angle to avoid multiple obstacles is

calculated from the edges of the circle as follows.

Obstacle Avoidance Guidance Law

To avoid multiple dynamic obstacles, the desired guidance law (heading angle) for equation (3) is defined as:

$$\psi_{dc}(t) = \text{atan2}\left((y_t - y),(x_t - x)\right) \pm \text{atan2}\left(R(t), d_s(t)\right). \tag{9}$$

We define the heading track error as $e(t) = \psi(t) - \psi_{dc}(t)$. Thus, the error dynamics become:

$$\dot{e}(t) = -c\psi(t) + c\tau(t) - \dot{\psi}_{dc}(t). \tag{10}$$

We propose the control law:

$$\tau(t) = \frac{1}{c}\dot{\psi}_{dc}(t) + \psi_{dc}(t),$$

to ensure the asymptotic stability of the heading track error dynamics (10).

3. 3. Decision Making Based on Risk Assessment

The control switches from target-reaching mode to obstacle avoidance mode if both of the following conditions are satisfied:

1. The waypoint LOS intersects with the adaptive velocity cone, causing the obstruction flag to be raised to one.
2. The risk index (RI) flag is one. The flag of the risk index (RI_{Flag}) is determined as:

$$\text{RI}_{\text{Flag}} = \begin{cases} 0, & \text{if RI} < C_{\text{t}}, \\ 1, & \text{if RI} \geq C_{\text{t}}. \end{cases} \tag{11}$$

where the risk index RI for DCPA, TCPA, and obstacle distance $\|D\|$ is defined as:

$$\text{RI} = \frac{1}{3}\left(F(\text{DCPA}) + F(\text{TCPA}) + F(\|\text{D}\|)\right), \tag{12}$$

with C_t being the threshold value of the risk index, and $F(\cdot)$ as defined in equation (13).

$$F(\zeta) = \begin{cases} 1, & \zeta \in [0, d_1], \\ 1 - 2\left(\frac{\zeta - d_1}{d_2 - d_1}\right)^2, & \zeta \in (d_1, \frac{d_1+d_2}{2}], \\ 2\left(\frac{\zeta - d_2}{d_2 - d_1}\right)^2, & \zeta \in (\frac{d_1+d_2}{2}, d_2], \\ 0, & \zeta \in (d_2, \infty). \end{cases} \tag{13}$$

where ζ represents DCPA, TCPA, or obstacle distance ($\|D\|$), and d_1, d_2 are tuning parameters for these metrics.

We define an additional flag called the "collision avoidance flag" (C_{Flag}). If the vehicle reaches the target, the mode switches to target-reaching mode and the collision avoidance mode is temporarily halted. We describe the switching logic as follows:

$$\text{C}_{\text{Flag}} = \begin{cases} 0, & \text{if no collision is detected}, \\ 1, & \text{if collision is detected}. \end{cases} \tag{14}$$

4. RESULTS AND DISCUSSION

In this section, we provide an overview of the simulation outcomes resulting from the implementation of the proposed algorithm in complex scenarios.

For the scenario, the MR begins at the coordinates $p_s(0) = [0,0]^\top$, with an initial heading angle of zero degrees ($\psi(0) = 0^\circ$) and a velocity $v_s = 0.16$ kilometers per hour. The designated waypoint is located at $p_t = (50,0)$ meter (m), and the velocity of all three dynamic obstacles is $v_o = 0.1$ kilometers per hour. The risk assessment parameters are set as follows: $C_{\text{t}} = 0.35$, DCPA $\in [10,25]$ meter, TCPA $\in [2,4]$ minutes, and obstacle distance $\|D\| \in [10,25]$ m.

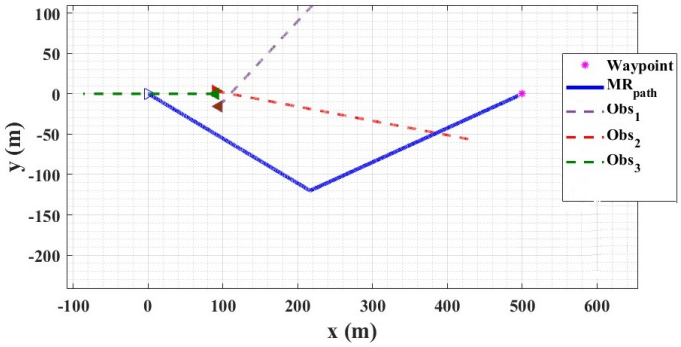

Fig. 4. Path of the MR and three dynamic obstacles.

4. 1. Discussion

Figure 4 illustrates the MR's trajectory for a specific scenario, using the proposed AVO algorithms. The results show that the MR successfully reaches the waypoint. Figure 5 provides the distances between the MR and obstacles using AVO methods. It is evident that the AVO algorithm successfully navigates the MR to the waypoint while avoiding all three obstacles.

Finally, Figure 6 shows the MR's heading angle and the corresponding control commands. These results demonstrate the effectiveness of the proposed algorithm in space vechicels collision avoidance.

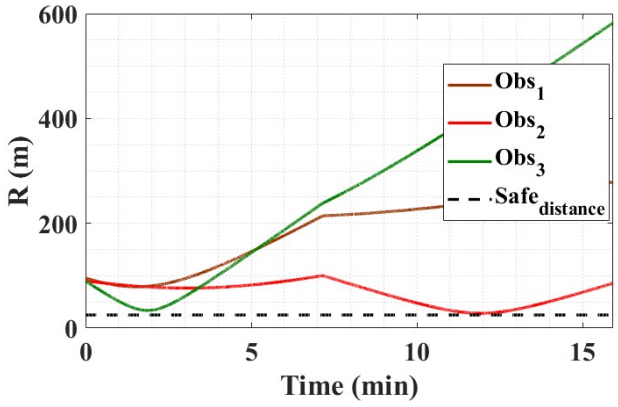

Fig. 5. Obstacles' distance.

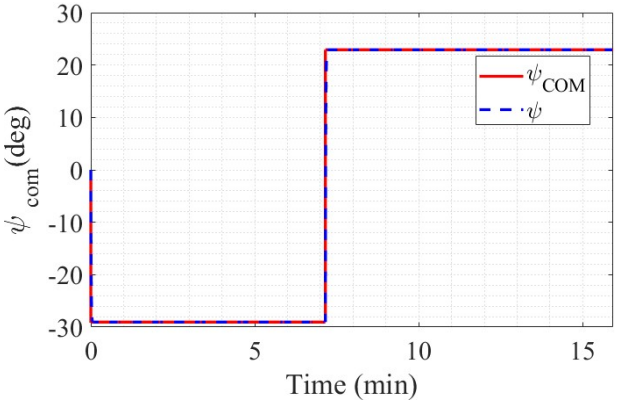

Fig. 6. MR heading angle and control command.

5. CONCLUSION

In this paper, we presented an adaptive velocity obstacle algorithm combined with a LOS guidance law for safe multi-vessel encounters while reaching a waypoint. We constructed an adaptive velocity cone from the MR to the unsafe set (circle) of multiple dynamic obstacles, utilizing the time to closest point of approach (TCPA) and distance to closest point of approach (DCPA) of each obstacle relative to the Mars rover. Future research will focus on extending the algorithm to account for MR and obstacle dynamics under disturbances and uncertainties, as well as formally characterizing the conditions under which the proposed method can be considered probabilistically safe.

CONFLICT OF INTERESTS

No conflict of interest has been expressed by the authors.

REFERENCES

[1] K. Ahmadi, D. Asadi, A. Merheb, S. Y. Nabavi-Chashmi, and O. Tutsoy, "Active fault-tolerant control of quadrotor UAVs with nonlinear observer-based sliding mode control validated through hardware in the loop experiments," *Control Engineering Practice*, vol. 137, 2023, Art. no. 105557, https://doi.org/10.1016/j.conengprac.2023.105557.

[2] K. Ahmadi, D. Asadi, S. Y. Nabavi-Chashmi, and O. Tutsoy, "Modified adaptive discrete-time incremental nonlinear dynamic inversion control for quad-rotors in the presence of motor faults," *Mechanical Systems and Signal Processing*, vol. 188, 2023, Art. no. 109989, https://doi.org/10.1016/j.ymssp.2022.109989.

[3] K. Ahmadi Dastgerdi, F. Pazooki, and J. Roshanian, "Model reference adaptive control of a small satellite in the presence of parameter uncertainties," *Scientia Iranica*, vol. 27, no. 6, pp. 2933-2944, 2020, (in Persian), https://doi.org/10.24200/sci.2019.50455.1704.

[4] M. Navabi and H. Ghanbari, "Attitude control of spacecraft using L1 Aadaptive control in the presence of actuator and disturbances," *Journal of Space Science and Technology*, vol. 13, no. 2, pp. 79-86, 2020, (in Persian), https://doi.org/10.30699/jsst.2020.2110.

[5] M. Navabi and N. Safaei Hashekvaei, "Kinematic modelling without singularity and nonlinear control of satellite attitude using direct adaptive and fuzzy PD control methods," *Journal of Space Science and Technology*, vol. 14, no. 2, pp. 77-88, 2021, (in Persian), https://doi.org/10.22034/jsst.2021.1248.

[6] D. Asadi, K. Ahmadi, S.Y. Nabavi Chashmi, and O. Tutsoy, "Controlability of multi-rotors under motor fault effect," *Artibilim: Adana Alparslan Turkes Bilim ve Teknoloji Universitesi Fen Bilimleri Dergisi*, vol. 4, no. 2, pp. 24-43, 2021.

[7] M. Navabi and P. Zarei, "Attitude nonlinear predictive control of an under actuated spacecraft," *Journal of Space Science and Technology*, vol. 14, no. 4, pp. 77-83, 2021, (in Persian), https://doi.org/10.22034/jsst.2021.1304.

[8] K. A. Dastgerdi, B. Singh, W. Naeem, and N. Athanasopoulos, "Adaptive velocity obstacle avoidance for multi-vessel encounters," in *UKACC 14th International Conference on Control (CONTROL)*, Winchester, United Kingdom, 2024, pp. 90-95, https://doi.org/10.1109/CONTROL60310.2024.10532047.

[9] S. Y. Nabavi Chashmi, D. Asadi, and K. Ahmadi Dastgerdi, "Safe land system architecture design of multi-rotors considering engine failure," *International Journal of Aeronautics and Astronautics*, vol. 3, no. 1, pp. 7-19, 2022, https://doi.org/10.55212/ijaa.1032693.

[10] T. I. Fossen and K. Y. Pettersen, "On uniform semiglobal exponential stability (USGES) of proportional line-of-sight guidance laws,"

Automatica, vol. 50, no. 11, pp. 2912-2917, 2014, https://doi.org/10.1016/j.automatica.2014.10.018.

[11] R. Polvara, S. Sharma, J. Wan, A. Manning, and R. Sutton, "Obstacle avoidance approaches for autonomous navigation of unmanned surface vehicles," *Journal of Navigation*, vol. 71, no. 1, pp. 241-256, 2018, https://doi.org/10.1017/S0373463317000753.

[12] K. A. Dastgerdi, B. Singh, W. Naeem, N. Athanasopoulos, and B. Lecallard, "Uncertainty aware path planning and collision avoidance for marine vehicles," *IFAC-PapersOnLine*, vol. 58, no. 20, pp. 235-240, 2024, https://doi.org/10.1016/j.ifacol.2024.10.060.

[13] K. A. Dastgerdi, B. Singh, N. Athanasopoulos, W. Naeem, and B. Lecallard, "Geometric path planning for high speed marine craft," *IFAC-PapersOnLine*, vol. 56, no. 2, pp. 5729-5734, 2023, https://doi.org/10.1016/j.ifacol.2023.10.525.

[14] P. Sarhadi, W. Naeem, and N. Athanasopoulos, "An integrated risk assessment and collision avoidance methodology for an autonomous catamaran with fuzzy weighting functions," in *UKACC 13th International Conference on Control (CONTROL)*, Plymouth, United Kingdom, 2022, pp. 228-234, https://doi.org/10.1109/Control55989.2022.9781453.

[15] Z. Liu, Y. Zhang, X. Yu, and C. Yuan, "Unmanned surface vehicles: An overview of developments and challenges," *Annual Reviews in Control*, vol. 41, pp. 71-93, 2016, https://doi.org/10.1016/j.arcontrol.2016.04.018.

[16] Z. Zhu, Y. Yin, and H. Lyu, "Automatic collision avoidance algorithm based on route-plan-guided artificial potential field method," *Ocean Engineering*, vol. 271, 2023, Art. no. 113737, https://doi.org/10.1016/j.oceaneng.2023.113737.

[17] M. Srinivasan and S. Coogan, "Control of mobile robots using barrier functions under temporal logic specifications," *IEEE Transactions on Robotics*, vol. 37, no. 2, pp. 363-374, 2021, https://doi.org/10.1109/TRO.2020.3031254.

[18] A. Singletary, K. Klingebiel, J. Bourne, A. Browning, P. Tokumaru, and A. Ames, "Comparative analysis of control barrier functions and artificial potential fields for obstacle avoidance," in *International Conference on Intelligent Robots and Systems (IROS)*, Prague, Czech Republic, 2021, pp. 8129-8136, https://doi.org/10.1109/IROS51168.2021.9636670.

[19] M. Hoy, A. S. Matveev, and A. V. Savkin, "Algorithms for collision-free navigation of mobile robots in complex cluttered environments: A survey," *Robotica*, vol. 33, no. 3, pp. 463-497, 2015, https://doi.org/10.1017/S0263574714000289.

[20] K. D. Do, "Synchronization motion tracking control of multiple underactuated ships with collision avoidance," *IEEE Transactions on Industrial Electronics*, vol. 63, no. 5, pp. 2976-2989, 2016, https://doi.org/10.1109/TIE.2016.2523453.

[21] M. Kamel, J. Alonso Mora, R. Siegwart, and J. Nieto, "Robust collision avoidance for multiple micro aerial vehicles using nonlinear model predictive control," in *International Conference on Intelligent Robots and Systems (IROS)*, Vancouver, BC, Canada, 2017, pp. 236-243, https://doi.org/10.1109/IROS.2017.8202163.

[22] Y. T. Kang, W. J. Chen, D. Q. Zhu, and J. H. Wang, "Collision avoidance path planning in multi-ship encounter situations," *Journal of Marine Science and Technology*, vol. 26, 1026-1037, 2021, https://doi.org/10.1007/s00773-021-00796-z.

[23] Z. Du, V. Reppa, and R. R. Negenborn, "MPC-based COLREGS compliant collision avoidance for a multi-vessel ship-towing system," in *European Control Conference (ECC)*, Delft, Netherlands, 2021, pp. 1857-1862, https://doi.org/10.23919/ECC54610.2021.9655091.

[24] P. Sarhadi, W. Naeem, and N. Athanasopoulos, "A survey of recent machine learning solutions for ship collision avoidance and mission planning," *IFAC-PapersOnLine*, vol. 55, no. 31, pp. 257-268, 2022, https://doi.org/10.1016/j.ifacol.2022.10.440.

[25] S. Campbell, W. Naeem, and G. W. Irwin, "A review on improving the autonomy of unmanned surface vehicles through intelligent collision avoidance manoeuvres," *Annual Reviews in Control*, vol. 36, no. 2, pp. 267-283, 2012, https://doi.org/10.1016/j.arcontrol.2012.09.008.

[26] W. Zhang, S. Wei, Y. Teng, J. Zhang, X. Wang, and Z. Yan, "Dynamic obstacle avoidance for unmanned underwater vehicles based on an improved velocity obstacle method," *Sensors*, vol. 17, no. 12, 2017, Art. no. 2742, https://doi.org/10.3390/s17122742.

[27] G. A. Mercado Velasco, C. Borst, J. Ellerbroek, M. M. van Paassen, and M. Mulder, "The use of intent information in conflict detection and resolution models based on dynamic velocity obstacles," *IEEE Transactions on Intelligent Transportation Systems*, vol. 16, no. 4, pp. 2297-2302, 2015, https://doi.org/10.1109/TITS.2014.2376031.

[28] Z. Gyenes and E. G. Szadeczky Kardoss, "Motion planning for mobile robots using the safety velocity obstacles method," in *19th International Carpathian Control Conference (ICCC)*, Szilvasvarad, Hungary, 2018, pp. 389-394, https://doi.org/10.1109/CarpathianCC.2018.8473397.

[29] P. Fiorini and Z. Shiller, "Motion planning in dynamic environments using velocity obstacles," *International Journal of Robotics Research*, vol. 17, no. 7, pp. 760-772, 1998, https://doi.org/10.1177/027836499801700706.